SCIENTIFIC REPORTS

OPEN

Real-time observational evidence of changing Asian dust morphology with the mixing of heavy anthropogenic pollution

Received: 19 September 2016
Accepted: 28 February 2017
Published online: 23 March 2017

Xiaole Pan[1,2], Itsushi Uno[2], Zhe Wang[1,2], Tomoaki Nishizawa[3], Nobuo Sugimoto[3], Shigekazu Yamamoto[4], Hiroshi Kobayashi[5], Yele Sun[1], Pingqing Fu[1], Xiao Tang[1] & Zifa Wang[1]

Natural mineral dust and heavy anthropogenic pollution and its complex interactions cause significant environmental problems in East Asia. Due to restrictions of observing technique, real-time morphological change in Asian dust particles owing to coating process of anthropogenic pollutants is still statistically unclear. Here, we first used a newly developed, single-particle polarization detector and quantitatively investigate the evolution of the polarization property of backscattering light reflected from dust particle as they were mixing with anthropogenic pollutants in North China. The decrease in observed depolarization ratio is mainly attributed to the decrease of aspect ratio of the dust particles as a result of continuous coating processes. Hygroscopic growth of Calcium nitrate ($Ca(NO_3)_2$) on the surface of the dust particles played a vital role, particularly when they are stagnant in the polluted region with high RH conditions. Reliable statistics highlight the significant importance of internally mixed, 'quasi-spherical' Asian dust particles, which markedly act as cloud condensation nuclei and exert regional climate change.

Mineral dust is considered one of the key contributors to global aerosol loadings[1,2], and it disturbs the atmospheric radiative balance[3,4], affects nutrient supplies in the marine ecosystem[5,6], and superimposes detrimental health impacts[7]. In East Asia, industrial/polluted region is located on transport pathway of dust plume[8]. Dust particles normally mixed with substantial amounts of pollutants and served as a good carrier for long-range transport of anthropogenic pollutants. Numbers of previous studies using off-line sampling and electron microscopy inspection reported a visible coatings (i.e. sulfate, nitrate) on some individual dust particles that were collected not only in the polluted area[9,10] but also in the remote maritime environment[11]. A high spatial specificity for the composition and structure of dust particles with different degrees of aging has been archived[12,13]. Nevertheless, the off-line based analysis requires manual operation and is labor-intensive, which results in a relatively large uncertainty and poor statistics[14]. The depolarization ratio (defined as the ratio of *s*-polarized to *p*-polarized signals; see Method) of the oscillation direction of the electromagnetic wave of scattering light from the illuminated particle is an applicable surrogate to indicate the irregularity of the dust particles[15,16]. Theoretical calculation on ellipsoid particles indicated that depolarization ratio of particle decreased evidently as its aspect ratio (defined as ratio of the longest dimension to its orthogonal width) decrease, which provided the possibility to investigate the time-resolved morphological variability of dust particles as it mixed with anthropogenic pollutants. Lidar (acronym of Light Detection And Ranging) observation is a powerful tool and provides the overall aerosol depolarization of an aggregation of multiple particles at high temporal/spatial resolution[17,18], however its volume scattering measurement cannot distinguish the internal/external mixing state of particles clearly[19]. Therefore, the *in-situ* and real-time measurement of the polarization change of single particles is necessary to obtain a better

[1]Institute of Atmospheric Physics/Chinese Academy of Sciences, State Key Laboratory of Atmospheric Boundary Layer Physics and Atmospheric Chemistry, Beijing, 100029, China. [2]Research Institute for Applied Mechanics, Kyushu University, Kasuga, Fukuoka, 816–8580, Japan. [3]National Institute for Environmental Studies, Tsukuba, Ibaraki, 305–8506, Japan. [4]Fukuoka Institute of Health and Environmental Sciences, Daizaifu, 818–0135, Japan. [5]University of Yamanashi, Yamanashi, 400–0016, Japan. Correspondence and requests for materials should be addressed to X.P. (email: panxiaole@mail.iap.ac.cn)

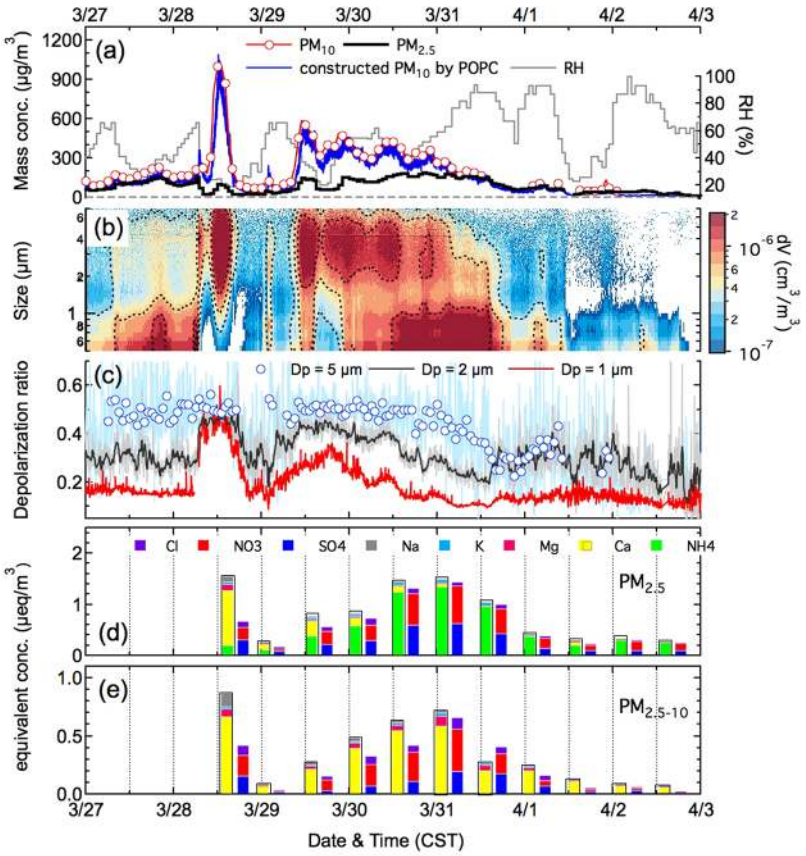

Figure 1. Time series of the observed mass concentration of $PM_{2.5}$, PM_{10} and constructed PM_{10} according to the POPC measurement, relative humidity (**a**), volume size distribution (**b**), hourly averaged depolarization ratio at Dp = 1 μm, 2 μm and 5 μm (**c**) and equivalent concentrations of identified water-soluble compounds in both the fine mode ($PM_{2.5}$) (**d**) and coarse mode ($PM_{2.5-10}$) (**e**) on the basis of filter-based chromatography analysis.

understanding of the mixing state of the dust particles, and there is no longer a need to presume the size distribution and morphology of the particles in optical models. A bench-top optical particle counter equipped with a depolarization module (Polarization Optical Particle Counter; POPC)[20] was recently developed and provides a size-resolved polarization study for individual particles[21,22]. Till now, there was no real-time measurement of morphological variations of dust particles in Beijing mega city, and the effect of neither chemical composition nor meteorology has been clarified.

A typical floating dust event was observed in North China on March 28–31, 2015. The main part of the dust plume originated from central Inner Mongolia and first arrived at a downtown area of Beijing mega city (observation site) on March 28. It was transported southerly to Shandong Province and dispersed into two parts (March 29). The northern half of the dust plume returned back and was stagnant over the Beijing area for approximately 3 days. This made the continuous observation of the same dust plume throughout the event possible. During dust event, we performed comprehensive measurements of the size distribution, polarization properties and chemical composition of aerosol particles. The purpose of this study is to quantitatively investigate morphological evolution of dust particles as mixing with pollutants, and to quantify the impact of both water-soluble inorganic (i.e. nitrate) and relative humidity (RH) on the formation of spherical dust particle in polluted area.

Results

The main dust plume first arrived at Beijing at 1200 CST (China Standard Time) on March 28, 2015. Mass concentrations of $PM_{2.5-10}$ (aerodynamic diameter of particles between 2.5 μm and 10 μm) increase sharply to 1049 μg/m^3, about tenfold that of $PM_{2.5}$ (aerodynamic diameter of particles less than 2.5 μm, 103 μg/m^3) (Fig. 1a and Fig. 1b). We selected particles at an optical size (D_p) of 5 μm to represent the dust particles[8,23], and fine mode particles at D_p = 1 μm for anthropogenic pollutants as references. During the onset of dust event, the uncontaminated dust particles were found to have a mean depolarization ratio of 0.5 ± 0.02 (Fig. 1c). The hourly averaged depolarization ratios of the particles at D_p = 1 μm increased significantly to 0.45 ± 0.01 due to the influence of fine non-spherical dust particles (Fig. 1c). With the transport of dust plume, mass concentration of $PM_{2.5-10}$ decreased significantly due to gravity settlement velocity and dilutions, whereas mass concentration of $PM_{2.5}$ gradually increased to 148 μg/m^3 at the end of the dust episode on March 31, as a result of production of secondary pollutants. The hourly averaged depolarization ratio of the dust particles decreased by approximately 46%, with a mean

of 0.34 ± 0.05, as dust particles were continuously mixed with secondary pollutants. Depolarization ratios of the particles at $D_p = 1\,\mu m$ and $D_p = 2\,\mu m$ decreased to their reference values of 0.1 ± 0.01 and 0.2 ± 0.03, respectively (Fig. 1c).

The equivalent concentration of water-soluble compositions on the filter samples in $PM_{2.5}$ (Fig. 1d) and $PM_{2.5-10}$ (Fig. 1e) showed that the ion balances were well achieved for nearly the entire period, except for the first onset of dust on March 28 when 97% of the particle mass in $PM_{2.5-10}$ was related to crustal matters with mass fraction of water-soluble Ca^{2+} (cCa^{2+}) less than 1% (Fig. 2a). On March 29, when the dust plume returned back to Beijing area (Fig. 2c), the mass concentrations of both the NO_3^- (cNO_3^-: 11.6 μg/m³) and cCa^{2+} (7.8 μg/m³) in $PM_{2.5-10}$ increased, suggested that the nitrate already started to accumulate due to absorption of nitric acid (HNO_3) on the surface of Ca-rich dust particles. In $PM_{2.5}$, secondary formation of water-soluble inorganic matter accounted for 44% of total $PM_{2.5}$, with high mass contributions of NO_3^- (fNO_3^-: 18.7 μg/m³) and SO_4^{2-} (fSO_4^{2-}: 14.0 μg/m³). After March 29 (Fig. 2d), the dust plume was stagnant over the Beijing area. NO_x emission in the city was mostly responsible for the significant enhancement of mass concentrations of fNO_3^- (44.9 μg/m³). Rapid increase of fSO_4^{2-} (30 μg/m³) may also attribute to preferential formation of sulfuric acid under the influence of both of NO_x[24] and dust[25]. In $PM_{2.5-10}$, mass concentrations of cNO_3^- (22.8 μg/m³) and cCa^{2+} (11.7 μg/m³) were also predominant. At the end of dust event on March 31 (Fig. 2e), the cCa^{2+} mass still accounted for 9% of total $PM_{2.5-10}$ mass, though its mass concentration was decreased 3.9 μg/m³, higher than that of cNO_3^- (2.9 μg/m³) and cSO_4^{2-} (3.1 μg/m³). Substantial coexistence of cCa^{2+} and cNO_3^- indicated of presence of deliquescent $Ca(NO_3)_2$, which formed by reaction between $CaCO_3$ and HNO_3 on the Ca-rich dust particles[26]. Almost no NH_4^+ (cNH_4^+) was found in $PM_{2.5-10}$. It was reasonable that preferential formation of $(NH_4)_2SO_4$ occurred at first in fine mode according to the good correlation ($r^2 = 0.94$) between SO_4^{2-} and NH_4^+. Because the Asian dust included substantial amount of calcium[23,27], reaction between $Ca(CO_3)_2$ and $(NH_4)_2SO_4$ on the surface of dust particles may result in the loss of NH_4^+ and the formation of insoluble $CaSO_4$[28].

Hourly averaged depolarization ratio of dust particles decreased as equivalent ratio of cNO_3^-/cCa^{2+} increased with a correlation coefficient $r^2 = 0.76$ (95% confidence interval, Fig. 3a). It indicated that, the more cNO_3^- mass present in the coarse mode, the more possibility to lead to the morphological change of dust particles due to heterogeneous reaction between $CaCO_3$ and HNO_3 on the dust particles in polluted urban area[26]. The formation of $Ca(NO_3)_2$ coating on the surface of dust particles reduced the critical super-saturation of dust particles and have strong potential to serve as CCN[29]. Impact of Na^+ (1.4%), Cl^- (0.8%) and K^+ (1.3%) in $PM_{2.5-10}$ on the decrease of depolarization ratio of dust particles were limited.

Morphological changes in dust particles were a synergistic effect of both pollutants and water content on the dust surface. Increase of relative humidity (RH) plays a vital role in decrease of the depolarization ratio of the dust particles in the presence of $Ca(NO_3)_2$ coating. The correlation coefficient between the depolarization ratio of the dust particles and the mass fraction of the aqueous content (water + Ca^{2+} + NO_3^-) in $PM_{2.5-10}$ was $r^2 = 0.66$ (95% confidence interval, Fig. 2b). Because all $Ca(NO_3)_2$ was deliquescent in the coarse mode when RH > 20% and underwent a exponential increase[30], the volume fraction of aqueous mass in the particles was calculated assuming density of dust particles of 2.5 g/cm³[31]. From March 29 to March 30, the ambient RH was $48 \pm 9\%$, the aqueous mass was estimated to be $28.5 \pm 10.8\,\mu g/m^3$, accounting for 17% of total volume in $PM_{2.5-10}$. However, at the end of dust episode on March 31, aqueous mass was $55.5 \pm 13.7\,\mu g/m^3$ on average, accounting for as high as 70% in the total volume of $PM_{2.5-10}$ at RH = 86%. Large fraction of aqueous matter well explained the obvious decrease in depolarization ratio of dust particles.

Although the observed depolarization ratio of the coated dust particles decreased evidently, we considered such dust particles as being 'quasi-spherical' because the observed minimal depolarization ratio (0.34) was still higher than that (0.08) of standard spherical particles (see Method). The polarization property of randomly oriented elongated ellipsoid particles was simulated on the basis of the T-matrix methodology[32,33]. A reception angle of 120 degrees relative to its incident light direction was the same with the POPC instrumentation. Theoretical calculation revealed that the depolarization ratio of dust particles was mainly determined by its aspect ratio (defined as the ratio of the longest dimension to its orthogonal width). Variations in the particle's refractive index (the real and imaginary part) can only explain limited depolarization variability (5%). As indicated in Fig. 4a, the observed maximal depolarization ratio (0.5) in this study corresponded to an aspect ratio of 1.7 for uncoated dust particles. During the polluted dust period on March 31, the aspect ratios of the dust particles were estimated to be 1.6 as the depolarization ratio of the dust particles decreased to 0.34, as shown by the yellow shading in Fig. 4a. Providing that the dust particles were in a standard ellipsoid configuration and underwent partial hygroscopic growth only at the shortest projection, a 70% increase in the volume of coating matter on the dust surface would cause the aspect ratio to decrease, at most, from 1.7 to 1.3. We concluded that, the moderate decrease in aspect ratio of the dust particle demonstrated that the deliquescent and hygroscopic processes of $Ca(NO_3)_2$ occurred on the entire surface of the dust particles. The depolarization ratio of the particles with $D_p = 1\,\mu m$ showed a linear decrease with increase of aspect ratio (Fig. 4b).

Discussion

Sulfate was frequently observed in the dust samples from Asian continent by electro-microscopy inspection[10,13]. In this study, a negative correlation ($r^2 = 0.75$, 95% confidence interval) between depolarization ratio of dust particles and mass fraction of cSO_4^{2-} in $PM_{2.5-10}$ was found. The good equilibrium in $PM_{2.5-10}$ implied that most of cSO_4^{2-} in the sample may formed as $CaSO_4$, the latter of which has small solubility (0.3%) and high deliquescent point (RH = 98%), and the large amount of cSO_4^{2-} in $PM_{2.5-10}$ was probably due to the significant dilution during the pretreatment of filter samples on the basis of ion chromatography analysis. In the real atmosphere, hygroscopic effect of $CaSO_4$ on the dust morphology seemed to be negligible. One of the possible explanation is the heterogeneous reaction itself may modify non-sphericity of dust particles, As demonstrated in laboratory experiment, chemical processes of sulfuric acid (H_2SO_4) on dust directly led to evident dust surface modifications[34];

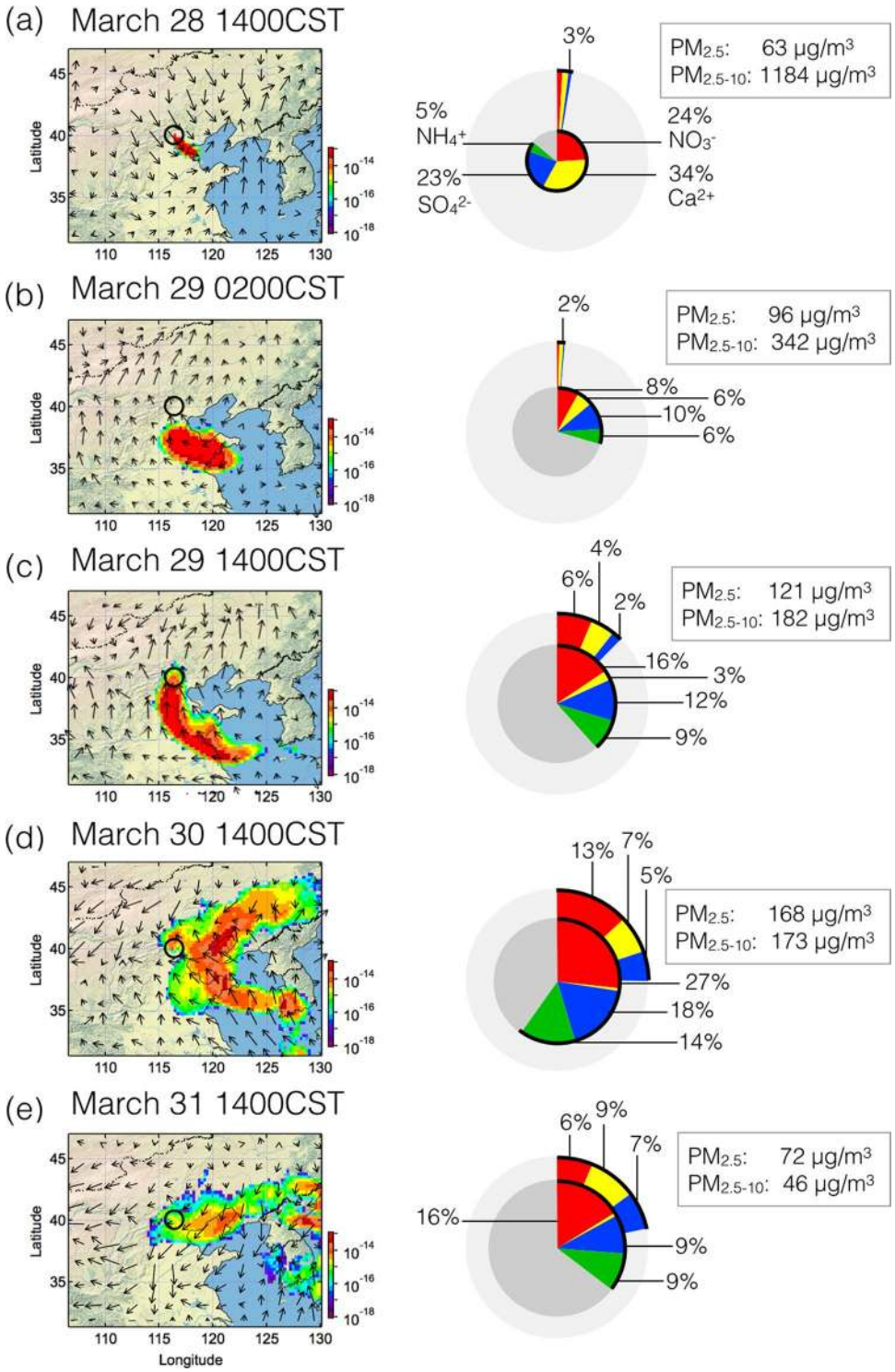

Figure 2. Footprint of the dust plume simulated by the HYSPLIT dispersion model ((**a**) detailed description of the simulation is shown in **Method**) during the dust-influencing period (on the left). The tracer particles were released from 500–1000 m above ground level at the observation site and dispersed for 5 days. The mass concentration of the particle (in mass/m^3) ranged from 0 to 1000 m every 3 hours. The figures on the right show corresponding mass concentrations of water-soluble inorganic matter (SO_4^{2-}: blue; NO_3^-: red; NH_4^+: green; and Ca^{2+}: yellow) in total $PM_{2.5}$ (inner Pi-chart) and $PM_{2.5-10}$ (outer gray ring). The maps were drawn by the software Igor Pro, http://www.wavemetrics.com/.

however direction conversion from $CaCO_3$ to $CaSO_4$ occurred more slowly and incomplete. Another contribution may rise from direct heterogeneous reaction between $CaCO_3$ and $(NH_4)_2SO_4$ at RH > 60% condition[28]. It

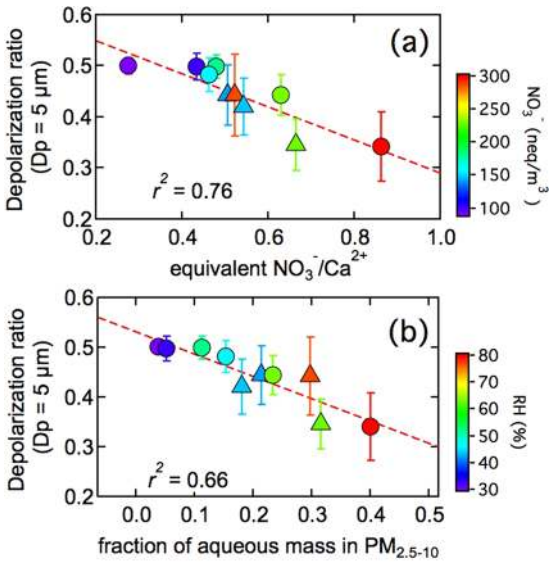

Figure 3. Relationship between the depolarization ratio of dust particles (Dp = 5 μm) and equivalent ratio of NO_3^-/Ca^{2+} (**a**) and the mass fraction of aqueous matter in the coarse mode (**b**). The colored circles in the plot represent the data during dust impact period from March 28 to April 1, 2015. The standard deviation (error bar) of depolarization ratio of dust particle was calculated for the dataset corresponding to filter sampling period. The color triangles indicate another weak floating dust case from April 9 to April 11, 2015. The backward trajectory analysis using HYSPLIT indicated that the air mass also came from northwest. Although none of the same dust plume was observed, the impact of anthropogenic pollutants on the depolarization ratio of the dust particle was similar.

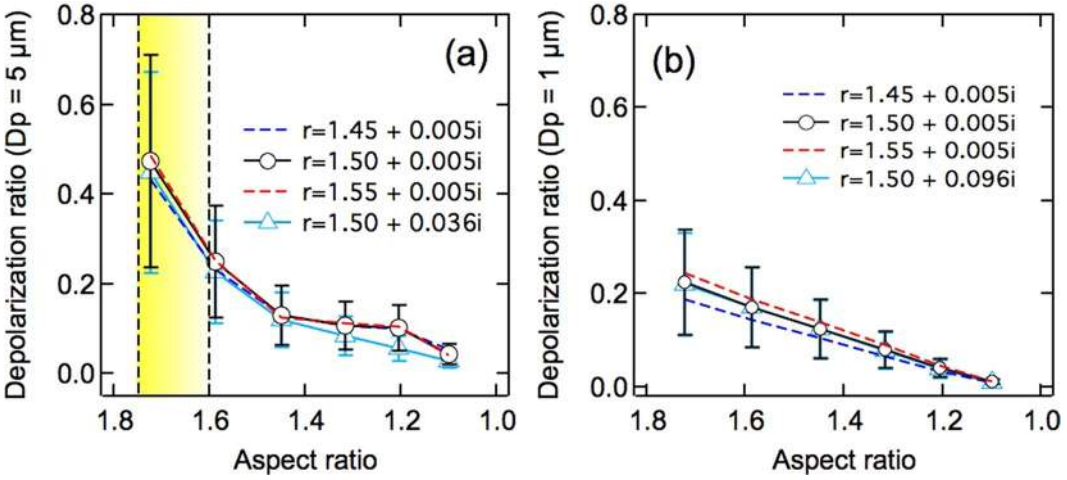

Figure 4. Theoretical simulation of the depolarization ratio of randomly oriented elongated ellipsoid particles as a function of the aspect ratio at Dp = 5 μm (**a**) and Dp = 1 μm (**b**) on the basis of the T-matrix methodology.

was worthy noting that mass concentration of cNO_3^- was much larger than cSO_4^{2-} in dust plume, with a cNO_3^-/cSO_4^{2-} mass ratio of 1.5–2.5, much higher than the value (0.16–0.5) reported ten years ago during the polluted dust period in Beijing[27]. It demonstrated that NO_x has exceeded SO_2 as the most important pollutant in Beijing area, in accordance with bottom-up emission inventory estimation[35]. Consequently, more direct absorption of reactive HNO_3 on the alkaline surface of dust particles becomes important to form strong hydrophilic compounds such as $Ca(NO_3)_2$ [29,36], the latter of which absorb water vapors at relative humidity (RH) above 10%[30], and apparently will affect to serve as cloud condensation nucleus (CCN).

Another important point, mineral dust and organic aerosols have traditionally been studied separately, however, more and more observations with a variety of means pointed out that adsorption of short-chain oxygenated hydrocarbons and low-vapor-pressure organic species (i.e. carboxylic acid) onto the dust surface cannot be overlooked[37–39]. For instance, shipboard aerosol time-of-flight mass spectrometer (ATOFMS) measurement of Asian aerosol outflow found that oxalic and malonic acids predominantly internally mixed with mineral dust, as a result of photochemical oxidation of volatile organic and diacids partitioning[40]. Quantitative analysis of

organic acid-related coating on the morphological alteration of mineral dust was limited. In the present study, dependence of depolarization ratio on organic matter in $PM_{2.5-10}$ remains unclear because of lacking of information of organic compound/function groups. During dust impact period, online measurement from Aerosol Chemical Speciation Monitor (Aerodyne Research, Inc.) at the site showed that mass concentration of organic matter accounted for ~40% of total mass in PM_1, indicating of substantial formation of secondary organic aerosol. Redistribution of semi-volatile organics from submicron to dust particles was likely happened for some organic acid with lower vapor pressure, in particular under higher ambient RH condition. Recent observation study in western Japan[22] using Aerosol Chemical Speciation Analyzer (Kimoto Electric Co., Ltd.) supported our speculations in this study, and pointed out that mass concentration of water-soluble organic carbon in coarse mode increased by a factor of three during a long lasting dust event.

This study, for the first time, investigated the real-time variation of depolarization property of dust particles as mixing with anthropogenic pollutants on the basis of newly developed polarization optical particle counter. The findings in this letter imply that the morphology of dust particles modified by internally mixing processes with water-soluble inorganic matters was statistically significant, and 'quasi-spherical' dust particle could substantially present in the polluted urban area, in particularly at high RH condition. The NO_x emissions in East Asia have been rapidly increasing over the last several decades[41], and the impact of nitrate on the morphology of coarse mode mineral dust and its subsequent spatial allocation have become increasingly important. These findings also provide new motivation to revisit decades of Lidar data[18] to provide a better understanding of the decadal variation in the changes in dust-pollution interactions against the background that anthropogenic emissions in East Asia have undergone profound changes[41]. This study also indicates the necessity of a reliable optical model of internally mixed polluted dust for a detailed analysis of polarization remote sensing observations.

Methods

Polarization Optical Particle Counter (POPC) and depolarization ratio. The POPC uses a 780 nm linearly polarized laser source and measures both forward and backward scattering intensity at 60 and 120 degrees relative to the direction of incident light. The polarization direction of the incident laser is parallel to the plane of the scattering angle. This configuration was optimized to reduce measurement uncertainty[20]. The depolarization ratio of the particles was defined as the ratio of the *s*-polarized to *p*-polarized signal (S/P) of the oscillation direction of the magnetic wave of scattering light from the particles. During the measurements, the pulse signals were sampled for 1 s and processed for 1.2 s. The sampling rate and half-width of full height (WHFH) of the POPC detector's output signal were 2×10^6 samples/s and approximately 35 μs, respectively. To avoid the coincidence error of the measurements, the inlet flow rate of POPC was set to 0.08 liters per minute (lpm) and was diluted with zero air (0.92 lpm, RH = 38 ± 1%). The residence time of diluted air mass was estimated to be 0.7 s, which was generally sufficient for aerosol particles to achieve equilibrium before measurement in the detecting chamber. It suggested that the wet particles tend to shrink due to loss of water. The measurement uncertainty in size determination was estimated to be 10–15%. Provided that the sampled particles are homogeneously distributed, the upper detection limit was estimated to be 6×10^5 particles per liter to fully meet the observation requirement. The optical size of the particle was converted from a forward scattering signal at 60 degree on the basis of the standard calibration curve, which was determined before the field campaign using standard spherical particles (Dynospheres, $D_p = 0.5$ μm, 1 μm, 3 μm, 5 μm, and 10 μm, JSR Life Sciences Corporation). Depolarization ratio of typical spherical particles at Dp = 3.344 μm (SS-033-P) and Dp = 5.124 μm (SS-053-P) were found to be 0.03 ± 0.01 and 0.07 ± 0.01, respectively. The instrument was installed at the top of a two-story building at the State Key Laboratory of Atmospheric Boundary Layer Physics and Atmospheric Chemistry (LAPC, Longitude: 116.3705E; Latitude: 39.9745 N), Institute of Atmospheric Physics/Chinese Academy of Sciences. Ambient air was drawn into the room through a 2-m-long vertical stainless steel tube (1/2 inch) with a laminar flow rate of 10 liters per minute. The turbulent loss of the coarse mode particles was limited.

Footprint simulation by HYSPLIT Dispersion Model. HYSPLIT, which is short for Hybrid Single Particle Lagrangian Integrated Trajectory Model, is a Lagrangian transport and dispersion model that is suitable for simulating long-range atmospheric transport processes (http://ready.arl.noaa.gov/HYSPLIT_disp.php). In this study, the meteorological field was the GDAS (Global Data Assimilation System, NCEP) dataset with time intervals of 3 hours (observation data at 00, 06, 12, and 18 UTC and forecast data at 03, 09, 15, and 21 UTC) and a spatial resolution of 1 degree by 1 degree. The inert particles were released below 1000 m and above ground level for 3 hours. The dry deposition process ($V_d = 0.5$ cm/s) was considered during the simulation. The spatial distribution of the footprint region of the air samples was calculated on the 5 days of forward simulation for 1 unit mass of particles released between 500 and 1000 m above ground level at the observation site. The mass concentration of the particles (in mass/m^3) at the surface was calculated by the HYPLIT dispersion model, considering large-scale convection, turbulent motions and the subgrid terrain effect in the simulation.

Filter sampling and Chromatographyh. The filter sampling in both $PM_{2.5}$ and PM_{10} were conducted on the LAPC campus from March 28 to April 12, 2015. Two aerosol samples were collected on quartz fiber filters (Pallflex) during both daytime (0800–1800 CST) and nighttime (1800–0800 CST) using a Hi-volume Air sampler (TISCH Environmental, Inc.) at a flow rate of 1 m^3/minute. The sampled filters were placed in a constant temperature (25 °C) and humidity (40%) chamber for 48 hours and weighed in the laboratory. The mass concentrations of the sampled aerosols (e.g., $PM_{2.5}$ and PM_{10}) on the filter were obtained according to the weight difference before and after sampling. The sampled filters were cut into 2-cm-diameter circular specimens and dissolved in 10 mL of deionized water, followed by 10-minute mechanical vibration and 10-minute ultrasonic wave stirring. Then, the solution was analyzed by IC techniques for anions F^-, Cl^-, NO_3^-, and SO_4^{2-} (ICS-1600, Thermo Fisher Scientific) and cations Na^+, NH_4^+, K^+, Mg^{2+}, and Ca^{2+} (ICS-1100, Thermo Fisher Scientific). In particular, for all

of the samples that were collected during heavy pollution periods, the solution was analyzed twice after undergoing dilutions of 2–5 times on the basis of the ambient mass concentration of $PM_{2.5}$. Both of the IC analyses were used for final data quality assurance, and the mass concentrations of SO_4^{2-}, NO_3^-, NH_4^+, and Cl^- showed good correlation with an online Aerosol Chemical Speciation Monitor (ACSM) measurement as shown in *SF.1*.

References

1. Pachauri, R. K. *et al.* Climate change 2014: synthesis Report. *Contribution of working groups I, II and III to the fifth assessment report of the intergovernmental panel on climate change* (IPCC, 2014).
2. Knippertz, P. & Stuut, J.-B. W. *Mineral Dust: A Key Player in the Earth System* (Springer, 2014).
3. Kaufman, Y. J., Tanré, D. & Boucher, O. A satellite view of aerosols in the climate system. *Nature* **419**, 215–223 (2002).
4. Uno, I. *et al.* Asian dust transported one full circuit around the globe. *Nature Geoscience* **2**, 557–560 (2009).
5. Jickells, T. D. *et al.* Global iron connections between desert dust, ocean biogeochemistry, and climate. *Science* **308**, 67–71 (2005).
6. Mahowald, N. M. *et al.* Observed 20th century desert dust variability: impact on climate and biogeochemistry. *Atmospheric Chemistry and Physics* **10**, 10875–10893 (2010).
7. Perez, L. *et al.* Coarse particles from Saharan dust and daily mortality. *Epidemiology* **19**, 800–807 (2008).
8. Zhang, X. Y. *et al.* Characterization of soil dust aerosol in China and its transport and distribution during 2001 ACE-Asia: 1. Network observations. *Journal of Geophysical Research: Atmospheres* 108 (2003).
9. Li, W. J. & Shao, L. Y. Observation of nitrate coatings on atmospheric mineral dust particles. *Atmospheric Chemistry and Physics* **9**, 1863–1871 (2009).
10. Matsuki, A. *et al.* Morphological and chemical modification of mineral dust: Observational insight into the heterogeneous uptake of acidic gases. *Geophysical research letters* 32 (2005).
11. Tobo, Y., Zhang, D., Matsuki, A. & Iwasaka, Y. Asian dust particles converted into aqueous droplets under remote marine atmospheric conditions. *Proceedings of the National Academy of Sciences* **107**, 17905–17910 (2010).
12. Deboudt, K. *et al.* Mixing state of aerosols and direct observation of carbonaceous and marine coatings on African dust by individual particle analysis. *Journal of Geophysical Research: Atmospheres* 115 (2010).
13. Kojima, T., Buseck, P. R., Iwasaka, Y., Matsuki, A. & Trochkine, D. Sulfate-coated dust particles in the free troposphere over Japan. *Atmospheric research* **82**, 698–708 (2006).
14. Gibson, E. R., Hudson, P. K. & Grassian, V. H. Aerosol chemistry and climate: Laboratory studies of the carbonate component of mineral dust and its reaction products. *Geophysical research letters* 33 (2006).
15. Sassen, K. *in Lidar* 19–42 (Springer, 2005).
16. Pan, X. *et al.* Polarization properties of aerosol particles over western Japan: classification, seasonal variation, and implications for air quality. *Atmos. Chem. Phys* **16**, 9863–9873 (2016).
17. Shimizu, A. *et al.* Continuous observations of Asian dust and other aerosols by polarization lidars in China and Japan during ACE-Asia. *Journal of Geophysical Research: Atmospheres* 109 (2004).
18. Shimizu, A. *et al.* Evolution of a lidar network for tropospheric aerosol detection in East Asia, Optical. *Engineering* **56**(3), 031219 (2016).
19. Hara, Y. *et al.* Asian dust outflow in the PBL and free atmosphere retrieved by NASA CALIPSO and an assimilated dust transport model. *Atmos. Chem. Phys* **9**, 1227–1239, doi:10.5194/acp-9-1227-2009 (2009).
20. Kobayashi, H. *et al.* Development of a polarization optical particle counter capable of aerosol type classification. *Atmospheric Environment* **97**, 486–492 (2014).
21. Sugimoto, N., Nishizawa, T., Shimizu, A., Matsui, I. & Kobayashi, H. Detection of internally mixed Asian dust with air pollution aerosols using a polarization optical particle counter and a polarization-sensitive two-wavelength lidar. *Journal of Quantitative Spectroscopy and Radiative Transfer* **150**, 107–113 (2015).
22. Pan, X. *et al.* Observation of the simultaneous transport of Asian mineral dust aerosols with anthropogenic pollutants using a POPC during a long-lasting dust event in late spring 2014. *Geophysical Research Letters* **42**, 1593–1598 (2015).
23. Mori, I., Nishikawa, M., Tanimura, T. & Quan, H. Change in size distribution and chemical composition of kosa (Asian dust) aerosol during long-range transport. *Atmospheric Environment* **37**, 4253–4263 (2003).
24. He, H. *et al.* Corrigendum: Mineral dust and NOx promote the conversion of SO2 to sulfate in heavy pollution days. *Scientific Reports* **4**, 6092, doi:10.1038/srep06092 (2014).
25. Nie, W. *et al.* Corrigendum: Polluted dust promotes new particle formation and growth. *Scientific Reports* **5**, 8949, doi:10.1038/srep08949 (2015).
26. Shi, Z. *et al.* Influences of sulfate and nitrate on the hygroscopic behaviour of coarse dust particles. *Atmospheric Environment* **42**, 822–827 (2008).
27. Sun, Y. *et al.* Chemical composition of dust storms in Beijing and implications for the mixing of mineral aerosol with pollution aerosol on the pathway. *Journal of Geophysical Research: Atmospheres* 110 (2005).
28. Tan, F. *et al.* Heterogeneous reactions of NO_2 with $CaCO_3$–$(NH_4)2SO_4$ mixtures at different relative humidities. *Atmos. Chem. Phys* **16**, 8081–8093, doi:10.5194/acp-16-8081-2016 (2016).
29. Sullivan, R. C. *et al.* Effect of chemical mixing state on the hygroscopicity and cloud nucleation properties of calcium mineral dust particles. *Atmos Chem Phys* **9**, 3303–3316 (2009).
30. Liu, Y. J., Zhu, T., Zhao, D. F. & Zhang, Z. F. Investigation of the hygroscopic properties of $Ca(NO_3)2$ and internally mixed $Ca(NO_3)2$/$CaCO_3$ particles by micro-Raman spectrometry. *Atmos Chem Phys* **8**, 7205–7215 (2008).
31. Reid, J. S. *et al.* Dynamics of southwest Asian dust particle size characteristics with implications for global dust research. *Journal of Geophysical Research: Atmospheres* 113 (2008).
32. Dubovik, O. *et al.* Application of spheroid models to account for aerosol particle nonsphericity in remote sensing of desert dust. *Journal of Geophysical Research: Atmospheres* **1984–2012**, 111 (2006).
33. Dubovik, O. *et al.* Non-spherical aerosol retrieval method employing light scattering by spheroids. *Geophysical Research Letters* 29 (2002).
34. Reitz, P. *et al.* Surface modification of mineral dust particles by sulphuric acid processing: implications for ice nucleation abilities. *Atmos Chem Phys* **11**, 7839–7858 (2011).
35. Wang, S. W. *et al.* Growth in NO x emissions from power plants in China: bottom-up estimates and satellite observations. *Atmos Chem Phys* **12**, 4429–4447 (2012).
36. Sullivan, R. C., Guazzotti, S. A., Sodeman, D. A. & Prather, K. A. Direct observations of the atmospheric processing of Asian mineral dust. *Atmos Chem Phys* **7**, 1213–1236 (2007).
37. Russell, L. M., Maria, S. F. & Myneni, S. C. B. Mapping organic coatings on atmospheric particles. *Geophysical Research Letters* 29 (2002).
38. Falkovich, A. H., Schkolnik, G., Ganor, E. & Rudich, Y. Adsorption of organic compounds pertinent to urban environments onto mineral dust particles. *Journal of Geophysical Research: Atmospheres* 109 (2004).
39. Gierlus, K. M., Laskina, O., Abernathy, T. L. & Grassian, V. H. Laboratory study of the effect of oxalic acid on the cloud condensation nuclei activity of mineral dust aerosol. *Atmospheric environment* **46**, 125–130 (2012).

40. Sullivan, R. C. & Prather, K. A. Investigations of the diurnal cycle and mixing state of oxalic acid in individual particles in Asian aerosol outflow. *Environmental Science Technology* **41**, 8062–8069 (2007).
41. Ohara, T. *et al.* An Asian emission inventory of anthropogenic emission sources for the period 1980 & ndash; 2020. *Atmos. Chem. Phys.* **7**, 4419–4444, doi:10.5194/acp-7-4419-2007 (2007).

Acknowledgements

This work was supported by the National Natural Science Foundation of China (Grant No. 41675128 and 41505115), and in part supported by MEXT/JSPS KAKENHI Grant JP25220101 from the Japan Society for the Promotion of Science (JSPS). The authors gratefully thank K. Osada and M. Uematsu for their valuable comments on the original manuscript.

Author Contributions

X.P., I.U. and Z.W. designed the entire study and coordinated all of the analyses. T.N. performed the T-Matrix model calculation and its related discussion. N.S. and H.K. examined the POPC data analyses. S.Y. supported the-chromatography chemical analysis. Y.S., P.F., Z.F.W., and X.T. supported the field observation in Beijing. X.P. and I.U. wrote the manuscript with valuable input from all of the co authors.

Additional Information

Supplementary information accompanies this paper at doi:10.1038/s41598-017-00444-w

Competing Interests: The authors declare that they have no competing interests.

Publisher's note: Springer Nature remains neutral with regard to jurisdictional claims in published maps and institutional affiliations.